Mode-Locking in a Network of Kuramoto-like Oscillators

Eugene Koskin[1], Dimitri Galayko[2], Orla Feely[1] and Elena Blokhina[1]
[1]University College Dublin, Ireland, [2]UPMC Sorbonne Universités, Paris, France

***Abstract*—In this paper we consider a network of phase oscillators. We develop the equations that model the time evolution of the phase of each oscillator in the network. The oscillator represents a modified Kuramoto oscillator and in this study we discuss how these modifications are obtained. In the context of this study, we use this network to model a network of PLLs for distributed clock applications. We analyse analytically and numerically the synchronisation modes of this system for different types of the coupling function. We show that depending on the properties of the coupling function, the network displays either multiple coexisting synchronisation modes or only a single synchronisation mode. While in the context of clock generation, multiple synchronisation modes coexisting in the system at the same parameters are a parasitic phenomenon. However in the context of other application such as associative memory models, mode-locking can be seen a useful phenomenon. The results provide a deeper understanding of globally synchronised clock networks with applications in microprocessor design.**

I. Introduction

A network of coupled oscillators is a very common model that allows one to describe complex phenomena in nature. Collective behaviour and synchronisation are observed and reported in engineering, physical, chemical and biological systems [1]–[17] including power networks, laser networks, superconductive Josephson junctions, circadian rhythm, associative memory, flashing of fireflies, periodical chemical reactions and many more.

In microprocessor engineering, a phase oscillator appears in clock generators. For example, a clock generating oscillator is one of the main components of all microprocessors. Typically a microprocessor contains one crystal oscillator that governs all elements and sub-systems through a clock distribution network. However, due to the complexity of microprocessor architectures and the increasing number of elements in them, it becomes more and more difficult to supply internal components with a clock signal. The clock distribution network required for modern microprocessors demands more energy and complicates design. The inability of a single oscillator to provide clocking for modern complex microsystems is the main motivation for the development of distributed clock networks.

One of the possible approaches to address this issue is to use so-called globally asynchronous locally synchronous (GALS) models [18]. Under this approach, a microprocessor or a complex microsystem consists of several synchronised areas or domains. All elements that belong to the same area are driven by their own clock and communicate to each other by means of a synchronous algorithm. The frequencies of the clocks in different areas are supposed to be different. GALS systems have a number of disadvantages such as a low communication rate between synchronised areas or communications errors that cannot be eliminated.

Since the studies of Pratt, Nguyen, Chandrakasan and Gutnik [19], [20], globally synchronous locally synchronous (GSLS) clock networks have been developed and studied intensively [18], [21]–[23]. In this approach, each clock that drives its designated area is represented by a phase locked loop (PLL) and can interact with its neighbours (fig. 1). As a result, the phase difference between two neighbour oscillators changes. A typical PLL consists of a voltage control oscillator (VCO), a phase detector (PD), a loop filter (LF) and a frequency divider (FD).

PLLs that are implemented using only digital components are called in this case all-digital phase locked loops (ADPLLs). Digital components allow one to easily integrate a clock network in the microprocessor architecture. In addition, the reference clock made of a crystal oscillator is more stable in comparison with the VCO in a PLL. It is known that GSLS systems achieve global synchronisation over a certain range of parameters, while in other cases these systems may display undesired synchronisation regimes called mode-locking.

In this paper we address the issue of synchronisation and mode-locking (undesired synchronised modes) and their stability in a clock network. We present a theoretical model for a network consisting of phase oscillators that model the behaviour of PLLs. We study a simple network of four oscillators to obtain analytical results and present numerical simulations for a larger network. As we shall show later in this paper, synchronisation modes and mode-locking strongly depend on the form of the transfer function that determines the nature of coupling between two neighbour oscillators.

The paper is organised as follows. in Section II we introduce the model of a single phase oscillator. We show that phase and frequency synchronisation occurs when a proportional-integral

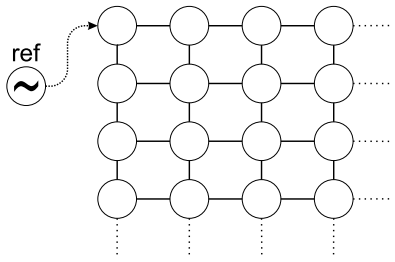

Fig. 1. Schematic clock network on Cartesian grid.

loop filter (PI) is implemented within a single oscillator. In Section III we extend our model to a four oscillator network. We show that depending on the transfer function and control parameters the system displays different types of stable co-existing synchronous modes. We discuss the extension of our model to a 3×3 Cartesian network by performing numerical simulation. Finally, Section IV summarises the results we have achieved.

II. Single Oscillator and Synchronisation with a Reference Signal

In this section we introduce the equation that describes the phase of a single oscillator driven by a harmonic reference signal. We start with a brief study of the single oscillator and we show that it is capable of synchronising with the reference signal both in terms of the phase, and frequency, when an integral path is included in the loop filter. This system is shown schematically in figure 2 and we use it to model a PLL. Later we will use this oscillator as a node for our network, however we will omit the index j for now.

A single phase oscillator has a central frequency ω and a reference input frequency Ω. These two signals serve as the input of the phase detector that calculates the transfer function $h(\Delta\varphi)$ whose argument is the phase difference $\Delta\varphi = \varphi_{ref}(t) - \varphi(t)$ between the reference phase φ_{ref} and the VCO phase φ. The output of the phase detector (the transfer function) is then passed to the proportional-integral controller (PI) denoted in the figure as the loop filter. The output of the PI, the signal v, controls then the frequency of the VCO. We can summarise this in the following equations

$$v = \mathrm{K}\dot{\psi}(t) + \mathrm{M}\psi(t), \tag{1}$$

$$\psi(t) = \int_0^t h\left(\varphi_{ref}(t') - \varphi(t')\right)\, dt', \tag{2}$$

$$\dot{\varphi}(t) = \omega + v\Delta\omega, \tag{3}$$

where K, M–gain factors for proportional and integral path in PI filter, ψ–accumulated phase error.

The loop filter output signal adjusts the local oscillator frequency in a linear way. All of this leads to a governing equation for a local clock of the form (3), where $\Delta\omega$ is the adjustment slope. For the remainder of this work we assume that $\Delta\omega > 0$ to simplify our analysis. Considering the

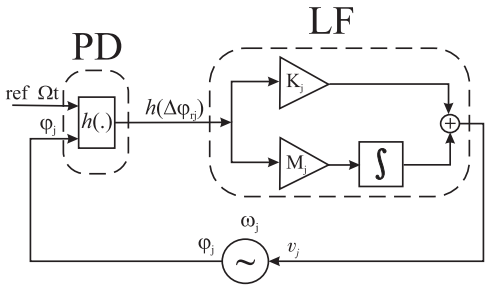

Fig. 2. Single phase-locked loop for local j-th oscillator.

particular case where the integral path is absent and $\mathrm{M} = 0$, we can find a simple governing equation from (1)-(3):

$$\dot{\varphi}(t) = \omega + \Delta\omega\mathrm{K}h\left(\Omega t - \varphi(t)\right), \tag{4}$$

where $\varphi_{ref}(t) = \Omega t$. One may notice when $h(x) = \sin(x)$, equation (4) transforms into the well known Kuramoto equation that can be found in a broad number of applications including high-power VCO design [13].

In order to analyze the asymptotic behavior of (4) we assume that the phase approaches a steady regime where the oscillator has a constant frequency and constant phase difference relative to the reference signal:

$$t \to \infty : \quad \varphi(t) = \tilde{\omega}t - \tilde{\varphi}, \tag{5}$$

where $\tilde{\omega}, \tilde{\varphi}$ are some constants. After substitution into (4) we will get definitions for $\tilde{\omega}, \tilde{\varphi}$ that corresponds to a stable asymptotic solution:

$$h(\tilde{\varphi}) = \frac{\Omega - \omega}{\Delta\omega\mathrm{K}}, \tag{6}$$

$$\tilde{\omega} = \Omega, \tag{7}$$

$$\Delta\omega\mathrm{K}h'(\tilde{\varphi}) > 0. \tag{8}$$

It can be seen that oscillator might be synchronized with external frequency Ω. The stable phase difference can be found from (6) under the condition (8). This phase difference is generally non-zero and depends upon system parameters ω, Ω, K.

In order to perform further analysis, we eliminate the integral in (1)–(3) by taking the derivative with respect to time:

$$\ddot{\varphi}(t) = \Delta\omega\mathrm{K}h'\left(\varphi_{ref}(t) - \varphi(t)\right)\left(\dot{\varphi}_{ref}(t) - \dot{\varphi}(t)\right) + \\ + \Delta\omega\mathrm{M}h\left(\varphi_{ref}(t) - \varphi(t)\right). \tag{9}$$

We want to note that the resulting equation is not the Kuramoto oscillator in its conventional form. So we refer to this equation as a Kuramoto-like oscillator since it contains some similar features. However, the transfer function h can be an arbitrary function and the equation contains an additional term. Now, let us substitute (5) into (9) in order to get corresponding stable asymptotic conditions for both proportional and integral path. After calculation one can obtain:

$$h(\tilde{\varphi}) = 0, \tag{10}$$

$$\tilde{\omega} = \Omega, \tag{11}$$

$$h'(\tilde{\varphi}) > 0, \mathrm{K} > 0, \mathrm{M} > 0 \text{ or} \\ h'(\tilde{\varphi}) < 0, \mathrm{K} < 0, \mathrm{M} < 0. \tag{12}$$

It can be seen that the fixed points are determined by (10) and depend only on the transfer function. Their stability depends on the slope of the transfer function and the gain factors of the loop filter. When $h(0) = 0, h'(0) > 0, \mathrm{K} > 0, \mathrm{M} > 0$ then the local oscillator synchronizes with the reference clock in both frequency and phase. For example, we can pick two different transfer functions such as:

$$h(x) = [(\pi + x) \mod 2\pi] - \pi, \tag{13}$$

$$h(x) = \sin(x). \tag{14}$$

Both of them lead to synchronisation, no matter what the initial conditions are. However, oscillator network modeled by such PD transfer functions demonstrate different behavior. They may exist in either a globally synchronised regime or a mode-locking regime. We will demonstrate this in the next section using an example of a four oscillator network connected in a chain.

III. Four coupled oscillators in a chain

In this section we analyze the phase synchronisation of an oscillator network with a periodic reference signal. We determine the conditions when a globally synchronized mode and a mode-locking regime can be observed.

A. Statement of the problem

For simplicity, let us consider a clock network which consists of four oscillators (fig. 3), where the first one is connected to stable reference clock. The first oscillator has three neighbours while all of the others have just two. In this case, each PLL consist of a VCO, a PI loop filter and N phase detectors connected in parallel. The number of phase detectors is equal to the number of neighbors in the vicinity of each VCO. The first oscillator has three neighbors where one of them is the reference clock, whereas the rest of the oscillators have only two neighbors. Each phase detector on fig. 4 is able to compare only one pair of phases. That's why two or more PD is needed for implementation in the network.

Each phase detector in figure 4 calculates the phase difference between neighbor and local clocks and maps it in accordance to transfer function $h(\Delta\varphi_{ij})$. Then, the signals from each local phase detector are summed together into one signal that goes to the PI filter which includes proportional and integral paths with gain factors $\mathrm{K}_j, \mathrm{M}_j$. Depending on an oscillator's position in the network, these factors may be different. However, here we use simple averaging $\mathrm{K}_j = \mathrm{K}/n_j, \mathrm{M}_j = \mathrm{M}/n_j$, where K, M are the same for all oscillators in the network, n_j – number of neighbors. Afterwards, the PI output signal v controls the frequency of the VCO in a linear way. Realistically, a control signal has its own minimum and maximum limits below or above which saturation takes place. In this research we assume that saturation does not occur.

Similar to (1)–(3) we write phase equations for our network,

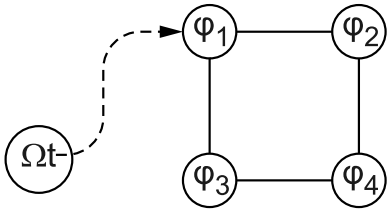

Fig. 3. Four oscillator chain network. The first oscillator connected to reference clock signal.

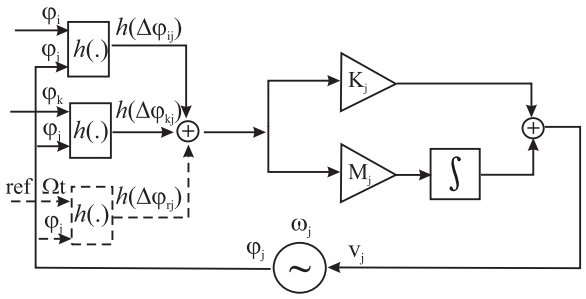

Fig. 4. PLL scheme for each node in clock network. Dashed phase detector corresponds to reference clock and embedded only in the first PLL.

where K denotes $\Delta\omega\mathrm{K}$ and M denotes $\Delta\omega\mathrm{M}$:

$$\dot{\varphi}_i = \omega_i + \frac{K}{n_i}\psi_i + \frac{M}{n_i}\int_0^t \psi_i(t')\,dt', \tag{15}$$

$$\psi_i = \sum_{j\in\mathbf{N}} h(\varphi_j - \varphi_i), \tag{16}$$

$$n_i = \{3, 2, 2, 2\}. \tag{17}$$

Here $i = \{1, 2, 3, 4\}$ denotes the number of an oscillator. Summation is performed over the number of topologically connected neighbors $\mathbf{N}$. For example, if $i = 1$ then:

$$\sum_{j\in\mathbf{N}} h(\varphi_j - \varphi_1) = h(\varphi_{ref} - \varphi_1) + h(\varphi_2 - \varphi_1) + h(\varphi_3 - \varphi_1),$$

where $\phi_{ref} = \Omega t$.

Lets eliminate the integral by differentiating, as we did previously:

$$\ddot{\varphi}_i = \frac{1}{n_i}\sum_{j\in\mathbf{N}}\Big(Kh'(\varphi_j - \varphi_i)(\dot{\varphi}_j - \dot{\varphi}_i) + Mh(\varphi_j - \varphi_i)\Big). \tag{18}$$

Now, we assume asymptotic solution $t \to \infty$, $\varphi_i(t) = \tilde{\omega}_i t - \tilde{\varphi}_i$. After substitution into (18) we get:

$$\sum_{j\in\mathbf{N}} h(\tilde{\varphi}_j - \tilde{\varphi}_i) = 0, \tag{19}$$

$$\tilde{\omega}_i = \Omega. \tag{20}$$

Equation (19) determines set of fixed points, where $\tilde{\varphi}_j - \tilde{\varphi}_i$ represents phase shift between j-th and i-th oscillators while their frequency is constant. In this case all oscillators frequency will be Ω. Notice that $\tilde{\varphi}_{ref} = 0$. We will discuss the issue of stability further using particular examples.

B. Coupling through a linear function

Assume that a phase detector can be described using a transfer function of the form (13). Such a PD includes information about both the sign and the absolute value of phase error and can be made from just a few XOR logic gates. First, we will find possible modes that can occur in our network and then we will check their stability.

In order to determine possible modes we substitute (13) into (19) and get a system of four nonlinear algebraic equations,

where $\tilde{\varphi}_{ref} = 0$:

$$\begin{cases} h(-\tilde{\varphi}_1) + h(\tilde{\varphi}_2 - \tilde{\varphi}_1) + h(\tilde{\varphi}_3 - \tilde{\varphi}_1) = 0, \\ h(\tilde{\varphi}_1 - \tilde{\varphi}_2) + h(\tilde{\varphi}_4 - \tilde{\varphi}_2) = 0, \\ h(\tilde{\varphi}_1 - \tilde{\varphi}_3) + h(\tilde{\varphi}_4 - \tilde{\varphi}_3) = 0, \\ h(\tilde{\varphi}_3 - \tilde{\varphi}_4) + h(\tilde{\varphi}_2 - \tilde{\varphi}_4) = 0. \end{cases} \tag{21}$$

Equations (21) are easy to solve with respect to $\tilde{\varphi}_1$. By taking into account the basic properties of $h(x)$ i.e. its oddness, 2π–periodicity and monotonicity we get

$$h(y) = h(x) \Rightarrow y = x + 2\pi n, n \in \mathbb{Z}.$$

Thus (21) becomes a system of linear algebraic equations:

$$\begin{cases} 2\tilde{\varphi}_2 - \tilde{\varphi}_4 = \tilde{\varphi}_1 + 2\pi n, \\ 2\tilde{\varphi}_3 - \tilde{\varphi}_4 = \tilde{\varphi}_1 + 2\pi m, \\ -\tilde{\varphi}_2 - \tilde{\varphi}_3 + 2\tilde{\varphi}_4 = 2\pi k. \end{cases} \tag{22}$$

The solution of (22) is:

$$\begin{cases} \tilde{\varphi}_2 - \tilde{\varphi}_1 = \frac{\pi}{2}\big(3n + m + 2k\big), \\ \tilde{\varphi}_3 - \tilde{\varphi}_1 = \frac{\pi}{2}\big(n + 3m + 2k\big), \\ \tilde{\varphi}_4 - \tilde{\varphi}_1 = \frac{\pi}{2}\big(2n + 2m + 4k\big), \end{cases} \tag{23}$$

where $n, m, k \in \mathbb{Z}$. Now we substitute (23) into (21.1) and find n, m, k such that $\tilde{\varphi}_1, \tilde{\varphi}_2, \tilde{\varphi}_3, \tilde{\varphi}_4 \in [0; 2\pi)$. Finally, we find three solutions which are possible under these constrains:

TABLE I
FIXED POINTS FOR LINEAR COUPLING FUNCTION ON TOPOLOGY GIVEN BY FIGURE 3

#	n	m	k	$\tilde{\varphi}_1$	$\tilde{\varphi}_2$	$\tilde{\varphi}_3$	$\tilde{\varphi}_4$
1	0	0	0	0	0	0	0
2	0	1	0	0	$\frac{\pi}{2}$	$\frac{3\pi}{2}$	π
3	1	0	0	0	$\frac{3\pi}{2}$	$\frac{\pi}{2}$	π

Let us check the stability of the modes in table I by applying a perturbation method: $\varphi_i(t) = \Omega t - \tilde{\varphi}_i + \delta_i(t)$. After substitution in (18) and taking account that $h'(x) = 1$ if $x \neq \pi n, n \in \mathbb{Z}$, we get system of equations that it is the same for all modes:

$$\begin{cases} \ddot{\delta}_1 = \frac{K}{3}\big(-3\dot{\delta}_1 + \dot{\delta}_2 + \dot{\delta}_3\big) + \frac{M}{3}\big(-3\delta_1 + \delta_2 + \delta_3\big), \\ \ddot{\delta}_2 = \frac{K}{2}\big(\dot{\delta}_1 - 2\dot{\delta}_2 + \dot{\delta}_4\big) + \frac{M}{2}\big(\delta_1 - 2\delta_2 + \delta_4\big), \\ \ddot{\delta}_3 = \frac{K}{2}\big(\dot{\delta}_1 - 2\dot{\delta}_3 + \dot{\delta}_4\big) + \frac{M}{2}\big(\delta_1 - 2\delta_3 + \delta_4\big), \\ \ddot{\delta}_4 = \frac{K}{2}\big(\dot{\delta}_2 + \dot{\delta}_3 - 2\dot{\delta}_4\big) + \frac{M}{2}\big(\delta_2 + \delta_3 - 2\delta_4\big). \end{cases} \tag{24}$$

This system of equation can be rewritten in the following vector form:

$$\dot{\mathbf{x}} = \mathbf{A}\mathbf{x}, \tag{25}$$

$$\mathbf{x} = (\dot{\delta}_1, \dot{\delta}_2, \dot{\delta}_3, \dot{\delta}_4, \delta_1, \delta_2, \delta_3, \delta_4)^{\mathrm{T}}, \tag{26}$$

$$\mathrm{A} = \begin{pmatrix} -K & \frac{K}{3} & \frac{K}{3} & 0 & -M & \frac{M}{3} & \frac{M}{3} & 0 \\ \frac{K}{2} & -K & 0 & \frac{K}{2} & \frac{M}{2} & -M & 0 & \frac{M}{2} \\ \frac{K}{2} & 0 & -K & \frac{K}{2} & \frac{M}{2} & 0 & -M & \frac{M}{2} \\ 0 & \frac{K}{2} & \frac{K}{2} & -K & 0 & \frac{M}{2} & \frac{M}{2} & -M \\ 1 & 0 & 0 & 0 & 0 & 0 & 0 & 0 \\ 0 & 1 & 0 & 0 & 0 & 0 & 0 & 0 \\ 0 & 0 & 1 & 0 & 0 & 0 & 0 & 0 \\ 0 & 0 & 0 & 1 & 0 & 0 & 0 & 0 \end{pmatrix} \tag{27}$$

The stability of (25) is determined by eigenvalues of matrix A. If the real parts of these eigenvalues are negative then (25) is stable. Eigenvalues are as follows:

$$\lambda_{1,2} = -K + \sqrt{K^2 - 4M}, \tag{28}$$

$$\lambda_{3,4} = -K - \sqrt{K^2 - 4M}, \tag{29}$$

$$\lambda^4 + 2K\lambda^3 + \left(\frac{K^2}{6} + 2M\right)\lambda^2 + \frac{KM}{3}\lambda + \frac{M^2}{6}. \tag{30}$$

It is straightforward to show that for (28), (29) $\mathrm{Re}(\lambda_{1,2,3,4}) < 0$ only if $K > 0, M > 0$. By applying Routh stability method to (30) we get condition for $\mathrm{Re}(\lambda_{5,6,7,8}) < 0$:

$$\begin{cases} (2K > 0) \wedge \left(\frac{K^2}{6} + 2M > 0\right), \\ \left(\frac{KM}{3} > 0\right) \wedge \left(\frac{M^2}{6} > 0\right), \\ 2K\left(\frac{K^2}{6} + 2M\right) > \frac{KM}{3}, \\ 2K\left(\frac{K^2}{6} + 2M\right)\frac{KM}{3} > (2K)^2\frac{M^2}{6} + \left(\frac{KM}{3}\right)^2. \end{cases} \tag{31}$$

The solution of (31) is the same as in the previous case. Therefore, all modes table (I) are stable only if $K > 0, M > 0$. The attracting mode depends on initial conditions.

For global clock synchronisation only one mode is acceptable where $\tilde{\varphi}_{1,2,3,4} = 0$. The other two modes cause undesirable mode-locking regimes.

C. Coupling through a sin-function

In this subsection we will show that mode-locking can be eliminated by an appropriate choice of the transfer function. This concept was studied in the Pratt and Nguyen paper [19] where they used a Hessian approach to prove the stability of fixed points. In our case, the oscillator network is determined by a system of differential equations. We study its stability by a reduction to the linear problem.

Let us use a phase detector describes by the transfer function (14). Such a phase detector can be found in analog phase detectors and power networks [9], [10], [13] . Due to sin-function coupling, governing equations (15) for such a case correspond to a modified Kuramoto model. But unlike an ordinary Kuramoto model, the integral path dramatically boosts synchronisation properties.

As we did previously, we will solve the system of algebraic equations (21.2)-(21.4) with respect to $\tilde{\varphi}_1$. Due to non-monotonicity of $h(x) = \sin(x)$ we will get:

$$h(y) = h(x) \Rightarrow \begin{cases} y = x + 2\pi n \\ y = -x + \pi + 2\pi n, \end{cases} \quad n \in \mathbb{Z} \tag{32}$$

This can be generalized in the form:

$$y = sx + (1 - s)\frac{\pi}{2} + 2\pi n, n \in \mathbb{Z}, s = \pm 1. \tag{33}$$

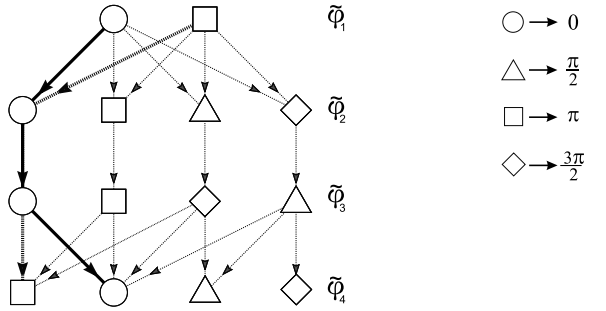

Fig. 5. Fixed points graph as the solution of problem (19), when $h(x) = \sin x$ and topology determined on figure 3. Thick lines represent stable modes. Solid thick lines correspond to domain $K > 0, M > 0$, dashed thick lines to $K < 0, M < 0$.

TABLE II
THE SOLUTION OF EQUATIONS (34)

#	s_n	s_m	s_k	$\frac{2}{\pi}(\tilde{\varphi}_2-\tilde{\varphi}_1)$	$\frac{2}{\pi}(\tilde{\varphi}_3-\tilde{\varphi}_1)$	$\frac{1}{\pi}(\tilde{\varphi}_4-\tilde{\varphi}_1)$
1	-1	1	-1	$-3-4k-2m-2n$	$-1-2m-2n$	$-1-2n$
2	-1	1	1	$-3+4k+2m-6n$	$-1-2m-2n$	$-1-2n$
3	1	-1	-1	$-1-2m-2n$	$1+4k-2m-2n$	$-1-2m$
4	1	-1	1	$-1-2m-2n$	$-3+4k-6m+2n$	$-1-2m$
5	1	1	1	$-2k-m-3n$	$-2k-3m-n$	$-2k-m-n$

Equations for fixed points determined from (19.2)-(19.4):

$$\begin{cases} -(1+s_n)\tilde{\varphi}_2 + s_n\tilde{\varphi}_4 = \gamma_n - \tilde{\varphi}_1, \\ -(1+s_m)\tilde{\varphi}_3 + s_m\tilde{\varphi}_4 = \gamma_m - \tilde{\varphi}_1, \\ s_k\tilde{\varphi}_2 + \tilde{\varphi}_3 - (1+s_k)\tilde{\varphi}_4 = \gamma_k, \end{cases} \quad (34)$$

$$\gamma_n = 2\pi n + \frac{\pi}{2}(1-s_n).$$

The solution of this with respect to $\tilde{\varphi}_1$, when determinant is nonzero present in table II.

By substitution in (19.1) we get an equation for $\tilde{\varphi}_1$. But, it is easy to see that $h(\tilde{\varphi}_{2,3} - \tilde{\varphi}_1) \in \{0, \pm 1\}$. This means that $h(\tilde{\varphi}_1) = 0, \pm 1, \pm 2$, where ± 2 does not provide a real solution because $h(x) \in [-1; 1]$. Due to $h(x) = \sin(x)$, we can denote: $\tilde{\varphi}_1 = \frac{\pi}{2}l$, where $l = l(k, m, n)$. Assuming $\tilde{\varphi}_{1-4} \in [0; 2\pi)$ we get a solution that consists of 20 modes. Such a set of modes takes a lot of space to place in a table, so we picture it in directed graph form in figure 5.

Each path in the graph represents the solution for a possible mode. By performing the same stability analysis as we did in the linear case, we found modes that are stable in some region of M, K. Thick solid line on the graph depicts stable solution when $K > 0, M > 0$ while thick dashed line – stable solution when $K < 0, M < 0$. All the rest modes are unstable for any K, M. Therefore, we showed that only one globally synchronized regime for our network exists when $K > 0, M > 0$.

D. Discussions

According to the results we have obtained in the previous section, we hypothesise that a PD based on monotonic functions on interval $x \in [-\pi; \pi)$ provide several possible modes in the network, while a PD based on non-monotonic functions realise only one mode. This mode corresponds to a globally synchronised network mode (GSM).

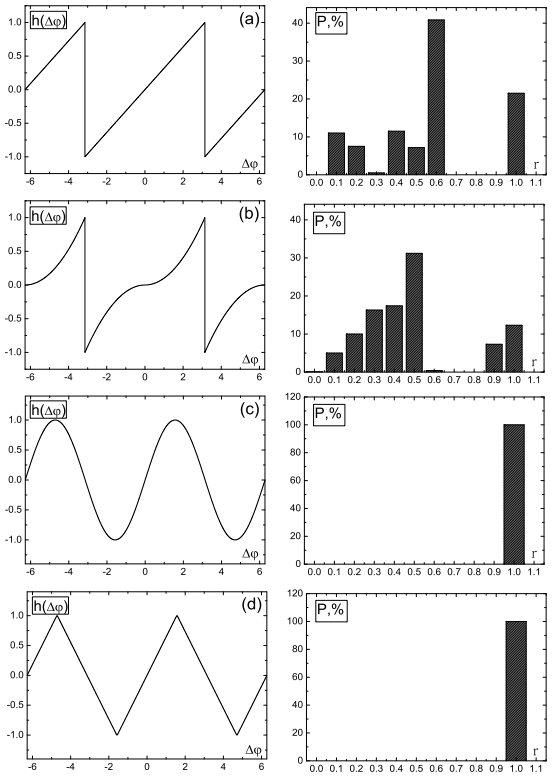

Fig. 6. The simulation results for 3×3 network and different transfer functions. Cases (c,d) correspond to global synchronisation mode.

In order to test our hypothesis we chose different transfer functions and extended our network to nine oscillators arranged into 3×3 Cartesian grid. Figure 6a represents the transfer function studied in Section III-B and figure 6c represents the one in Section III-C. Figures 6(b, d) represent additional transfer functions where figure 6b – monotonic function and figure 6d – non-monotonic.

To study synchronisation of the network, we used a complex order parameter that is inherent for the Kuramoto model [24]

$$re^{i\psi} = \left\langle e^{i\varphi_j} \right\rangle,$$

where $\langle\rangle$ denotes averaging over all oscillators in the network, $r \in [0; 1]$ – scalar order parameter measures the phase coherence, ψ – is the average phase. If the network is globally synchronised then when $t \to \infty$, $r(t) = 1$, whereas if it is fully out of sync then $r(t) = 0$. When the network stays in a mode-locking regime then $r(t)$ is constant and has a value between one and zero.

In the figure 6(a-d) we have presented a statistical distribution for the asymptotic value of order parameter r that was calculated under different initial conditions. They were chosen to cover all real initial phases that can be observed in reality. All initial phases in the network were unifor-

mally distributed within the interval $[0; 2\pi)$, but the initial frequency was kept constant for all oscillators. To simulate each distribution we used the same set of parameters: $\dot{\varphi}_j(0) = 2, \Omega = 1, K = 10, M = 10, N = 1000$, where N – number of trials.

Distributions of order parameter show that the transfer functions in figure 6(c, d) realise only one value for order parameter $r = 1$ under the initial conditions introduced above. This means that the network always approaches to GSM. In contrast, the distributions in figure 6(a, b) reveal the wide range of order parameters. It shows that mode locking regime in the network may occur with respect to initial conditions. Moreover, the slope of the transfer function is responsible for the probability of GSM. In particular, the transfer function (a) leads to GSM with probability $P = 22\%$, while transfer function (b) leads to GSM with probability $P = 12\%$.

IV. Conclusion

In this paper, we proposed the continuous model for coupled clock network in application to microprocessor design. Each node of the network represented through voltage controlled oscillator and connected with its neighbors on Cartesian grid. The interaction between oscillators was performed via their phase differences with a help of phase detector and proportional-integral filter. We showed that depending on phase detector's transfer function and filter parameters the oscillator network made of six or nine oscillators may approach to synchronised regime.

We analised conditions when the desired globally synchronised regime occur and found that our results are consistent with the Pratt and Nguyen paper [19]. However, due to description in terms of differential equation, our model implies an extension for noise implementation for jitter.

Acknowledgment

The authors gratefully acknowledge the support of Science Foundation of Ireland (SFI).

References

[1] Y. Wang, Y. Hori, S. Hara, and F. Doyle, "The collective oscillation period of inter-coupled Goodwin oscillators," in *Decision and Control (CDC), 2012 IEEE 51st Annual Conference on*, Dec 2012, pp. 1627–1632.

[2] M. Ciszak, F. Arecchi, S. Euzzor, and R. Meucci, "Experimental characterization of the dynamics in a network of chaotic FitzHugh-Nagumo neurons," in *Complexity in Engineering (COMPENG), 2014*, June 2014, pp. 1–6.

[3] T. d'Eysmond, A. D. Simone, and F. Naef, "Analysis of precision in chemical oscillators: implications for circadian clocks," *Physical Biology*, vol. 10, no. 5, p. 056005, 2013.

[4] Y. Li, Z. Liu, J. Luo, and H. Wu, "Coupling-induced synchronization in multicellular circadian oscillators of mammals," *Cognitive Neurodynamics*, vol. 7, no. 1, pp. 59–65, 2013.

[5] Gerasimos G. Rigatos and Efthymia G. Rigatou, "Synchronization of circadian oscillators and protein synthesis control using the derivative-free nonlinear Kalman filter," *Journal of Biological Systems*, vol. 22, no. 04, pp. 631–657, 2014.

[6] P. Sacre and R. Sepulchre, "Sensitivity analysis of oscillator models in the space of phase-response curves: Oscillators as open systems," *Control Systems, IEEE*, vol. 34, no. 2, pp. 50–74, April 2014.

[7] T. Petrič, A. Gams, A. J. Ijspeert, and L. Žlajpah, "On-line frequency adaptation and movement imitation for rhythmic robotic tasks," *The International Journal of Robotics Research*, vol. 30, no. 14, pp. 1775–1788, 2011.

[8] Y. Wang and F. J. Doyle III, "On influences of global and local cues on the rate of synchronization of oscillator networks," *Automatica*, vol. 47, no. 6, pp. 1236 – 1242, 2011, special Issue on Systems Biology.

[9] F. Dörfler and F. Bullo, "Synchronization and transient stability in power networks and nonuniform Kuramoto oscillators," *SIAM Journal on Control and Optimization*, vol. 50, no. 3, pp. 1616–1642, 2012.

[10] F. Dörfler, M. Chertkov, and F. Bullo, "Synchronization in complex oscillator networks and smart grids," *Proceedings of the National Academy of Sciences*, vol. 110, no. 6, pp. 2005–2010, 2013.

[11] F. Dörfler and F. Bullo, "Topological equivalence of a structure-preserving power network model and a non-uniform Kuramoto model of coupled oscillators," in *Decision and Control and European Control Conference (CDC-ECC), 2011 50th IEEE Conference on*, Dec 2011, pp. 7099–7104.

[12] B. Johnson, S. Dhople, A. Hamadeh, and P. Krein, "Synchronization of nonlinear oscillators in an LTI electrical power network," *Circuits and Systems I: Regular Papers, IEEE Transactions on*, vol. 61, no. 3, pp. 834–844, March 2014.

[13] Y. Tousi, O. Momeni, and E. Afshari, "A novel CMOS high-power terahertz VCO based on coupled oscillators: Theory and implementation," *Solid-State Circuits, IEEE Journal of*, vol. 47, no. 12, pp. 3032–3042, Dec 2012.

[14] A. Chepizhko and V. Kulinskii, "On the relation between Vicsek and Kuramoto models of spontaneous synchronization," *Physica A: Statistical Mechanics and its Applications*, vol. 389, no. 23, pp. 5347–5352, 2010.

[15] Y. Wang and F. Doyle, "Optimal phase response functions for fast pulse-coupled synchronization in wireless sensor networks," *Signal Processing, IEEE Transactions on*, vol. 60, no. 10, pp. 5583–5588, Oct 2012.

[16] L. Liu, J. Wu, and K. Tian, "A distributed synchronous clock for sensor networks," in *Wireless Communications and Signal Processing (WCSP), 2014 Sixth International Conference on*, Oct 2014, pp. 1–5.

[17] J. de Cos and A. Suarez, "Efficient simulation of solution curves and bifurcation loci in injection-locked oscillators," *Microwave Theory and Techniques, IEEE Transactions on*, vol. 63, no. 1, pp. 181–197, Jan 2015.

[18] E. Zianbetov, D. Galayko, F. Anceau, M. Javidan, C. Shan, O. Billoint, A. Korniienko, E. Colinet, G. Scorletti, J. Akré, and J. Juillard, "Distributed clock generator for synchronous SoC using ADPLL network," in *Custom Integrated Circuits Conference (CICC), 2013 IEEE*, Sept 2013, pp. 1–4.

[19] G. Pratt and J. Nguyen, "Distributed synchronous clocking," *Parallel and Distributed Systems, IEEE Transactions on*, vol. 6, no. 3, pp. 314–328, Mar 1995.

[20] V. Gutnik and A. Chandrakasan, "Active GHz clock network using distributed PLLs," *Solid-State Circuits, IEEE Journal of*, vol. 35, no. 11, pp. 1553–1560, Nov 2000.

[21] C. Shan, F. Anceau, D. Galayko, and E. Zianbetov, "Swimming pool-like distributed architecture for clock generation in large many-core SoC," in *Circuits and Systems (ISCAS), 2014 IEEE International Symposium on*, June 2014, pp. 2768–2771.

[22] J. Akré, J. Juillard, M. Javidan, E. Zianbetov, D. Galayko, A. Korniienko, and E. Colinet, "A design approach for networks of self-sampled all-digital phase-locked loops," in *Circuit Theory and Design (ECCTD), 2011 20th European Conference on*, Aug 2011, pp. 725–728.

[23] C. Shan, E. Zianbetov, M. Javidan, F. Anceau, M. Terosiet, S. Feruglio, D. Galayko, O. Romain, E. Colinet, and J. Juillard, "FPGA implementation of reconfigurable ADPLL network for distributed clock generation," in *Field-Programmable Technology (FPT), 2011 International Conference on*, Dec 2011, pp. 1–4.

[24] S. H. Strogatz, "From Kuramoto to Crawford: exploring the onset of synchronization in populations of coupled oscillators," *Physica D: Nonlinear Phenomena*, vol. 143, no. 1, pp. 1–20, 2000.